

Supporting Information

**Chiroptical Methods in a Wide Wavelength Range for Seeking Ln³⁺
Complexes with Circularly Polarized Luminescence of Practical Interest**

Marcin Górecki,^{a,b} Luca Carpita^a, Lorenzo Arrico^a, Francesco Zinna^a and Lorenzo Di Bari^{a*}

^a Dipartimento di Chimica e Chimica Industriale, Università di Pisa, via Moruzzi 13,
56124 Pisa, Italy. E-mail: lorenzo.dibari@unipi.it

^b Institute of Organic Chemistry, Polish Academy of Sciences, ul. Kasprzaka 44/52,
01-224 Warsaw, Poland.

Conformational analysis and chiroptical properties of ligands: *i*Pr-PyBox and Ph-PyBox

In the first step conformational search at molecular mechanics level (see Experimental section) was done for an arbitrary chosen (*R,R*)-configuration of *PyBox* ligands, and then DFT geometry optimizations were carried out to find a reliable set of the most populated conformers in solution and their relative energies. We used the ω B97X-D/6-311+G(d,p) level of theory with the polarizable continuum model (PCM), which demonstrates a very good balance between short computational time and high accuracy. We ran DFT optimizations using the PCM for CH₃OH ($\epsilon = 32.63$) and CHCl₃ ($\epsilon = 4.9$) to reflect better the measurement conditions of ECD and VCD spectra, respectively.

The conformational search for (*R,R*)-*i*PrPyBox indicated the presence of 8 stable conformers within a 3 kcal/mol energy range; within conformers with population $\leq 3\%$ we took into consideration only one structure (Figure S1). As expected, the structure of the most abundant conformers (#1-6), which cover $\sim 97\%$, indicated the same arrangements of the two oxazoline rings, in which three nitrogen atoms are lying in the same plane. The relatively high number of conformers with small differences in energies are linked with the presence of various rotamers in *i*Pr- moiety in the two oxazoline rings. It is worth to notice that in equilibrium there is also negligible amount of conformers with the different arrangements of the oxazoline rings (#7-8) in which only two nitrogen atoms are lying on the same line. The PCM model indicates the presence of a slightly different population of all conformers in CH₃OH, however still the differences in the range of 1 kcal/mol are related only to the stabilization of conformations with differences in the *i*Pr- moiety, but the set of rings remains identical.

In the same energy range for (*R,R*)-PhPyBox there are 3 stable conformers (Figure 2, bottom) with different arrangement of rings. They have more pronounced difference in population in two solvents used for calculations, among which the most abundant one (#1) covers in CHCl₃ $\sim 85\%$ and in CH₃OH $\sim 62\%$ of overall. The remaining higher-energy conformers (#2 and #3) are much more stabilized in CH₃OH and cover $\sim 38\%$ of overall, while in CHCl₃ only $\sim 16\%$.

UV and ECD spectra of (*R,R*)-*i*PrPyBox and (*R,R*)-PhPyBox were measured in CH₃OH solution (Figure S2). UV spectra show two resolved bands centered at ~ 285 nm and at ~ 250 nm (Figure S2, left) which have different intensities. In coherence with the absorption there are ECD bands; they show a positive Cotton Effect (CE) at ~ 285 nm, very well resolved for (*R,R*)-PhPyBox, followed by a second more intense positive one at ~ 245 nm for (*R,R*)-*i*PrPyBox and at ~ 235 nm for (*R,R*)-PhPyBox. The ECD bands for (*R,R*)-PhPyBox are ~ 2.6 times more intense with respect to its *i*Pr- analog, while in the terms of $|g_{abs}|$, this difference is lower (1×10^{-3} and 5×10^{-4} , respectively). As we shall see later on, these factors are pretty small, especially when we consider Ln³⁺ complexes based on these chiral auxiliaries. Apart from these differences, as mentioned before, the ECD and UV spectra have a rather similar profile, which is perhaps not surprising, since the lowest energy conformers are in line. They are governed by π - π^* pyridine transition mixed with n - π^* transitions coming from oxazolines. Moreover, in the case of (*R,R*)-PhPyBox there is also strong overlap with π - π^* transitions of phenyl substituent which results in a substantial increase of the intensity of all electronic bands.

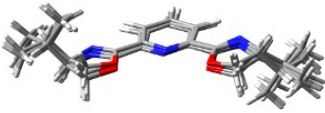
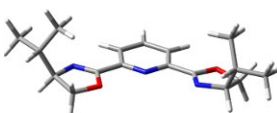
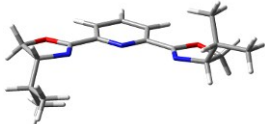
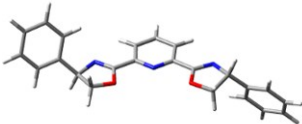
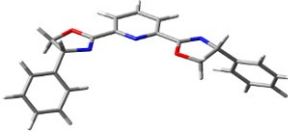
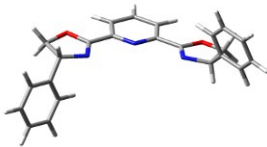
(<i>R,R</i>)-<i>i</i>Pr-PyBox			
			
	Conf. #1-6	Conf. #7	Conf. #8
	in CHCl₃		
Pop. [%]	96.4%	3.22 %	0.34 %
ΔE [kcal/mol]	0.00-0.42 kcal/mol	1.13 kcal/mol	2.47 kcal/mol
	in CH₃OH		
Pop. [%]	91.3%	6.7 %	2.0 %
ΔE [kcal/mol]	0.00-0.72 kcal/mol	0.83 kcal/mol	1.54 kcal/mol
(<i>R,R</i>)-Ph-PyBox			
			
	Conf. #1	Conf. #2	Conf. #3
	in CHCl₃		
Pop. [%]	84.5	14.3	1.2
ΔE [kcal/mol]	0.00	1.05	2.52
	in CH₃OH		
Pop. [%]	61.6	29.8	8.6
ΔE [kcal/mol]	0.00	0.43	1.17

Figure S1. The overview of stable conformers of (*R,R*)-*i*PrPyBox and (*R,R*)-PhPyBox. Relative energies (ΔE) and populations at 298 K ($\geq 1\%$) is based on DFT-optimized conformers within 3 kcal/mol calculated at the ω B97X-D/6-311+G(d,p) level of theory using PCM for CHCl₃ and CH₃OH.

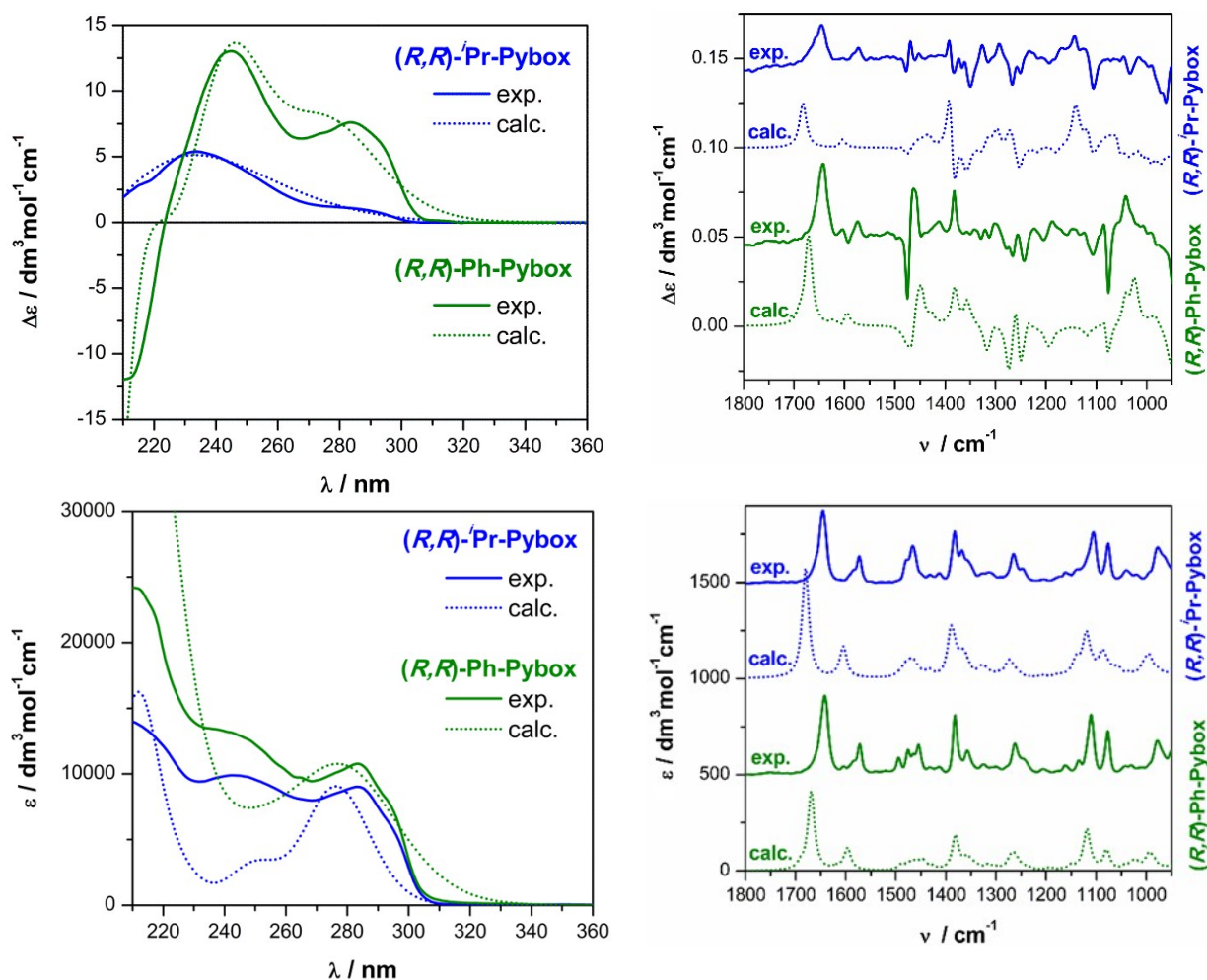


Figure S2. Left: TDDFT simulated ECD/UV spectra of (R,R) -*i*PrPyBox and (R,R) -PhPyBox compared to experimental spectra recorded in CH_3OH . Calculations ran with CAM-B3LYP/def2-TZVP/PCM/ CH_3OH ; spectra red-shifted by 20 nm, Gaussian band-width 0.98 eV and 0.43 eV, respectively. **Right:** DFT simulated VCD/IR spectra of (R,R) -*i*PrPyBox and (R,R) -PhPyBox compared with experimental spectra recorded in CDCl_3 . Calculations run at the $\omega\text{B97X-D}/6\text{-}311\text{+G(d,p)}/\text{PCM}/\text{CHCl}_3$; frequencies scaled by a factor 0.970; Lorentzian band-width $\sigma = 8 \text{ cm}^{-1}$. All spectra are shown as a vertical offset for better clarity with normalized intensity.

In the next step of our chiroptical analysis, the set of conformers found were submitted for calculations of chiroptical properties. ECD and UV spectra were simulated using TDDFT method at the CAM-B3LYP/def2-TZVP/PCM/ CH_3OH level of theory. The comparisons of the experimental and calculated ECD/UV spectra are presented in Figure S2. The computed spectra show perfect agreement with the experimental data recorded in CH_3OH , and in both cases reproduce the whole spectral range, confirming *ipso facto* the absolute configuration to be (R,R) and that the right set of conformers have been found in the conformation analysis step.

IR and VCD spectra of (R,R) -*i*PrPyBox and (R,R) -PhPyBox were collected in CDCl_3 solution and they are shown in Figure S2 (right) together with the Boltzmann averaged calculated spectra at the $\omega\text{B97X-D}/6\text{-}311\text{+G(d,p)}/\text{PCM}/\text{CHCl}_3$ level. Moreover, in Figure 9 (main text) we presented the VCD/IR spectra of (S) -enantiomers, which are in very good

mirror-image relationship. Basically, IR spectra of the *PyBox* (*i*Pr- vs. Ph-) ligands keep very similar profile; the only noticeable difference may be found in the range 1500-1450 cm⁻¹ where the pyridine and -CH₂- vibrations from oxazolines are overlapped with C-H aliphatic banding and C-C stretching vibrations appearing from *i*Pr- or Ph- groups, respectively. Analogously, VCD spectra of **(*R,R*)-*i*PrPyBox** and **(*R,R*)-PhPyBox** have pretty similar pattern, however, in the case of **(*R,R*)-PhPyBox** the intensity of most of bands are different with respect to **(*R,R*)-*i*PrPyBox**, in particular the most highlighted ones arising in 1500-1450 cm⁻¹ range. The comparison of the experimental and calculated IR and VCD spectra shows a very good consistency, both in terms of reproducing signs in the amide stretching vibrations (~1650 cm⁻¹) and *fingerprint* region (1500-950 cm⁻¹) part of spectra. Furthermore, the relative intensity of bands are computed well.

Summarizing, the chiroptical properties of **(*R,R*)-*i*PrPyBox** and **(*R,R*)-PhPyBox** are in line, and the differences are featured only mainly in the intensity of ECD bands. The good agreement between the experimental and calculated spectra confirms the correctness of our stereochemical investigations derived from ECD and VCD spectra.

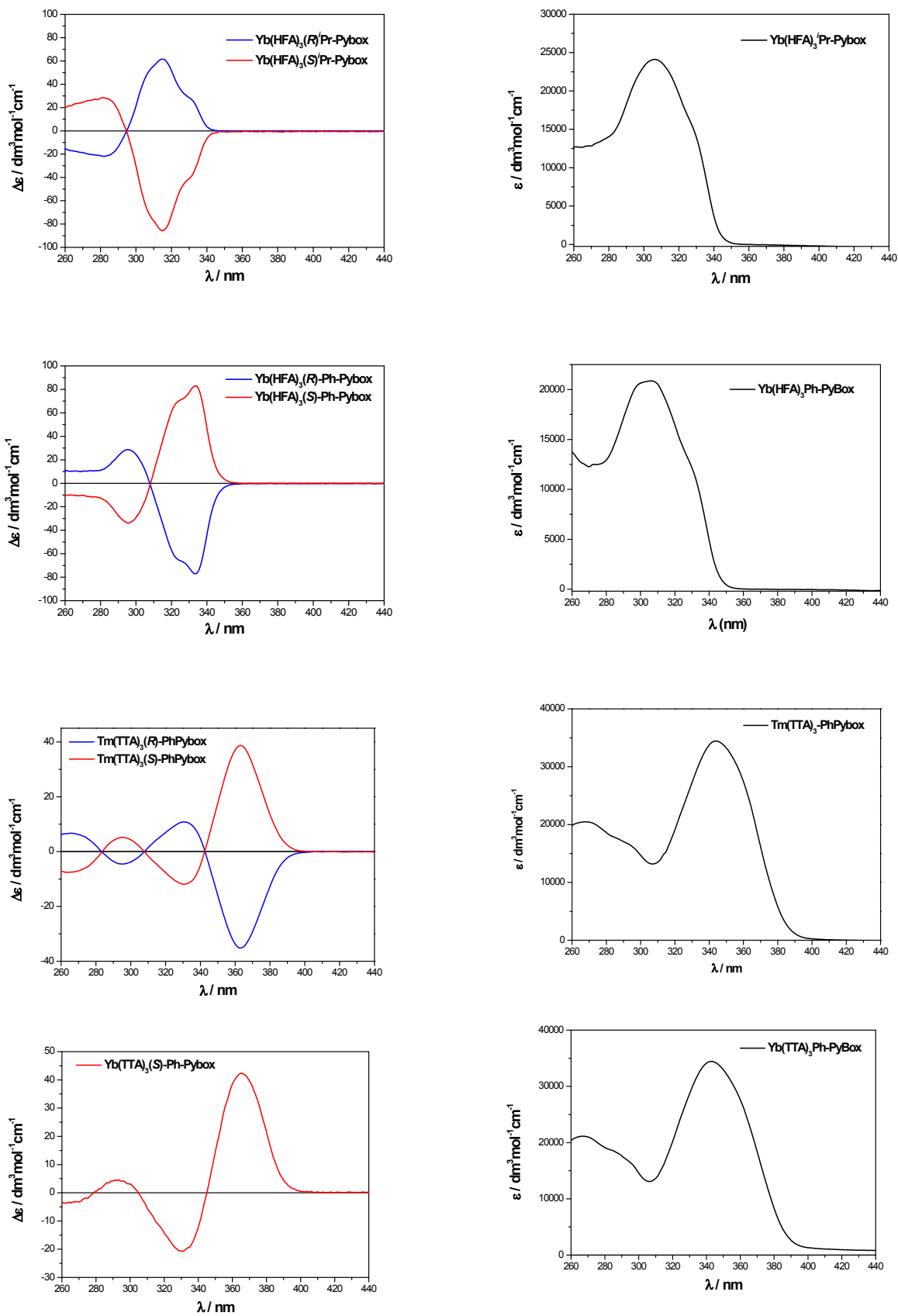


Figure S3. ECD (left) and UV (right) spectra of Ln^{3+} complexes recorded in CH_2Cl_2 ($c \sim 0.4$ mM).

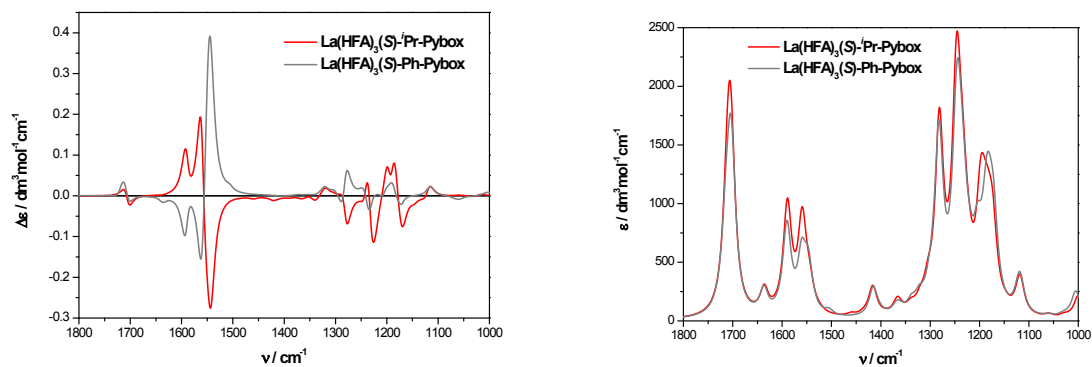


Figure S4. DFT calculated VCD (left) and IR (right) spectra for $\text{La}(\text{HFA})_3(\text{S})\text{-PhPyBox}$ compare to $\text{La}(\text{HFA})_3(\text{S})\text{-}i\text{PrPyBox}$; calculations run at the B3LYP functional, and 6-31G(d) basis set for H, C, N, O, F and the LanL2DZ for La; frequencies are not scaled; Lorentzian band-width $\sigma = 10 \text{ cm}^{-1}$.

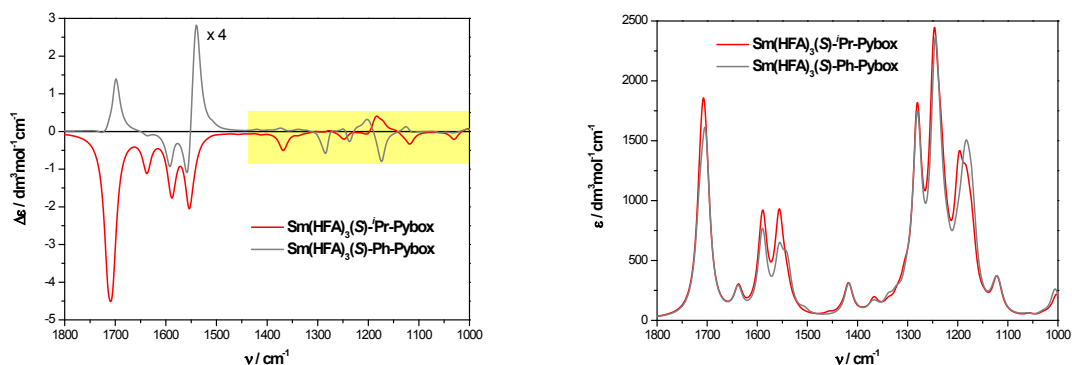


Figure S5. DFT calculated VCD (left) and IR (right) spectra for $\text{Sm}(\text{HFA})_3(\text{S})\text{-PhPyBox}$ compare to $\text{Sm}(\text{HFA})_3(\text{S})\text{-}i\text{PrPyBox}$; calculations run at the B3LYP functional, and 6-31G(d) basis set for H, C, N, O, F and the SDD for Sm; frequencies are not scaled; Lorentzian band-width $\sigma = 10 \text{ cm}^{-1}$; for better comparison the VCD spectrum of $\text{Sm}(\text{HFA})_3(\text{S})\text{-PhPyBox}$ was multiplied by 4.